Journal of Microbiological Methods 87 (2011) 49–55

Contents lists available at ScienceDirect

Journal of Microbiological Methods

journal homepage: www.elsevier.com/locate/jmicmeth

Monitoring the in situ crystallization of native biopolyester granules in *Ralstonia eutropha* via infrared spectroscopy

Michael Porter, Jian Yu *

Hawai'i Natural Energy Institute, University of Hawai'i at Mānoa, 1680 East West Road, POST 109, Honolulu, HI, 96822, USA

ARTICLE INFO

Article history:
Received 4 September 2010
Received in revised form 28 June 2011
Accepted 6 July 2011
Available online 23 July 2011

Keywords:
Biopolyester granules
FTIR
In situ crystallization
Instantaneous crystallinity
PHB

ABSTRACT

Poly(3-hydroxybutyrate) (PHB), a representative polyhydroxyalkanoate (PHA), is a naturally occurring biopolyester stored as tiny, intracellular granules in microbial cells. In vivo, native PHB granules are amorphous, stabilized by a monolayer membrane and intra-granule water. When subjected to varying environmental conditions, the native granules may become partially crystalline. The in situ crystallinity of native PHB granules in *Ralstonia eutropha* cells suspended in aqueous solution was monitored with attenuated total reflectance Fourier transform infrared spectroscopy (ATR-FTIR). No sample preparation was required for measurement. A major measurement error could be caused by the evaporation of water. Therefore, the infrared absorption spectra should be taken after the initial settlement of cells, but before excessive dehydration. Background interference caused by water and non-PHB biomass was constant throughout the time course of measurement, regardless of granule crystallinity. The wavenumber 1184 cm^{-1} was found to be most sensitive to the in situ crystallinity of native PHB granules.

1. Introduction

Microbial biopolyesters have gained much attention as eco-friendly alternatives to petrochemical-based plastics because they are biodegradable and can be produced from renewable feedstocks. One class of biopolyester with many potential environmentally friendly applications is polyhydroxyalkanoate (PHA). The most widely studied, representative form of PHA and focus of this work is poly(3-hydroxybutyrate) (PHB).

PHB is synthesized and stored as tiny, intracellular inclusion body granules (0.2–0.5 μm in diameter) by a wide variety of bacterial species as carbon and energy reserves (Anderson and Dawes, 1990; Byrom, 1994). In vivo, PHB granules are fully amorphous, contain a small amount of intra-granule water (5–10%), and are surrounded by a monolayer membrane composed of phospholipids and proteins (Barnard and Sanders, 1989; Horowitz and Sanders, 1994; Sudesh et al., 2000). Purified PHB, on the other hand, becomes a semi-crystalline (50–70%) material (Gunaratne et al., 2004). To recover PHB for commercial applications, the granules must be separated from the cells and purified. During recovery processes the environment of the granules changes, causing PHB to undergo varying degrees of irreversible crystallization (Barnard and Sanders, 1989; Horowitz and Sanders, 1994; Sudesh et al., 2000). Little is known about the in situ crystallization of PHB granules in their native form under changing environmental conditions. This information is important to develop more efficient recovery methods and reduce the production costs of PHA.

There are several methods to measure polymer crystallinity. Popular methods include: x-ray diffraction (XRD), differential scanning calorimetry (DSC), and attenuated total reflectance Fourier transform infrared spectroscopy (ATR-FTIR) (Barham et al., 1984; Gunaratne et al., 2004; Smith, 1999). Monitoring the instantaneous crystallinity of biopolyesters in their native aqueous environment, however, is difficult via XRD and DSC because of demands on material purity and dryness. ATR-FTIR is particularly useful for in situ measurements because no such sample preparation is necessary (Smith, 1999). That is, the infrared absorption spectra of PHB-containing cells in an aqueous solution can be measured directly to determine the instantaneous crystallinity of the native PHB granules without purifying or drying the PHB.

ATR-FTIR is an efficient analytical tool used to measure the chemical composition and structural arrangement of local molecular environments within solid, liquid, gas, semi-solid, and polymeric samples (Smith, 1999). When infrared light interacts with a polymer the energy is absorbed causing molecular vibrations at wavenumbers specific to its chemical bonds. In polyesters, for instance, two spectral regions are characteristic. The carbonyl group (C═O) absorbs infrared light around 1800–1600 cm^{-1} and the ester backbone (C–O–C) absorbs infrared light around 1300–1000 cm^{-1} (Smith, 1999). Conformational changes in a sample, such as melting and crystallization, can be seen as an increase, decrease, or shift in the characteristic absorption bands (Smith, 1999). Consequently, the infrared spectrum of PHB is information rich,

* Corresponding author. Tel.: +1 808 956 5873; fax: +1 808 956 2336.
E-mail address: jianyu@hawaii.edu (J. Yu).

0167-7012/$ – see front matter © 2011 Elsevier B.V. All rights reserved.
doi:10.1016/j.mimet.2011.07.009

providing a quick and convenient method to monitor conformational changes in PHB, such as crystallization.

The crystallization of pure PHB describing the material transition from an amorphous melt to a semi-crystalline solid has been studied by many research groups (Barham et al., 1984; Gunaratne et al., 2004; Padermshoke et al., 2005; Sato et al., 2004; Xu et al., 2002; Zhang et al., 2005). When pure PHB is heated above its melting point (~180 °C) it exists as an amorphous entanglement of loosely packed molecules (Barham et al., 1984). Upon cooling, the PHB molecules crystallize, aligning into tightly packed helical chains, forming lamellar sheets and/or spherulites (Barham et al., 1984). The proposed crystal structure of PHB consists of two antiparallel, left-handed 2_1-helices (Cornibert and Marchessault, 1975; Padermshoke et al., 2005; Sato et al., 2004). The driving force behind the energetically favorable process is thought to be C–H···O hydrogen bonding between the C═O and CH_3 groups in PHB (Furukawa et al., 2005; Sato et al., 2004; Zhang et al., 2005). During the crystallization process, the molecular mobility of the PHB molecules becomes restricted due to chain folding and close packing into a crystalline state. Conversely, melting PHB causes the C–H···O hydrogen bonds to weaken, increasing molecular mobility.

In contrast to purified PHB, the amorphousness of native PHB granules in vivo is stabilized by proteins, lipids, and water (Barnard and Sanders, 1989; Horowitz and Sanders, 1994; Sudesh et al., 2000). Structural proteins, known as phasins, and lipids contained in the granule membrane may play a role in regulating or stabilizing the amorphous granules (Grage et al., 2009; Stuart et al., 1998; Sudesh et al., 2000). More importantly, the 5–10% of intra-granule water present in the granules is thought to act as a plasticizer, forming hydrogen bonds (C–H···OH_2···O) with the carbonyl groups of the polyester backbones in PHB (Sudesh et al., 2000). This phenomenon prevents strong dipole–dipole interactions from occurring between the C═O and CH_3 groups in PHB (Sudesh et al., 2000). Removal of the intra-granule, PHB-bound water promotes in situ crystallization due to increased C–H···O hydrogen bonding, analogous to the cooling crystallization process in pure PHB (Sudesh et al., 2000). When monitoring the infrared absorption spectra of PHB-containing cells in an aqueous solution, these impurities (i.e. non-PHB biomass and water) may generate considerable background noise and spectral interference. Moreover, evaporation of water during the measurement may cause the granules to crystallize. Hence, the infrared absorption spectra may not reflect the true, instantaneous crystallinity of PHB in vivo.

In this work, we developed the first known method to monitor the instantaneous crystallinity of native PHB granules in *Ralstonia eutropha*, a representative bacterial microorganism containing PHA, suspended in an aqueous solution. Spectral interference from background absorptions caused by water and other non-PHB cellular components were observed and accounted for in the measurements at specific wavenumbers. This paper reports the details of the in situ method and provides a quantitative description of the true, instantaneous crystallinity of PHB granules by correlating ATR-FTIR spectral measurements with DSC crystallinity measurements. Although this paper is specific to PHB granules contained in *R. eutropha* cells, the method outlined here may prove useful as a framework to monitor the in situ crystallization of biopolyesters in microorganisms similar to *R. eutropha*.

2. Material and methods

2.1. Materials

In this work, *R. eutropha* cells containing 60 wt.% PHB were stored at room temperature (~23 °C) in a solution of 0.2 M H_2SO_4 (pH 2) as a slurry of 250 g cell mass/L. The acidic condition (pH 2) was used to stop possible microbial activity in the aqueous solution, a standard method used in water sampling and preservation. In the acidic solution, the cells exhibited no biological activity and the PHB granules remained mostly intact in their native amorphous state. A slurry density of 250 g cell mass/L provided the most optimal working conditions for the in situ measurements that were dependent on water evaporation and cell sedimentation rates. Three aqueous solutions of the PHB-containing cells were prepared from the slurry for controlled samples of different crystallinity: (1) *native PHB granules*, suspended in acidic solution as described above; (2) *centrifuged PHB granules*, where the solution of native granules was spun at 10,000 g for 1 h and resuspended in the supernatants solution; and (3) *heated PHB granules*, where the solution of native granules was heated at 140 °C for 2 h and set at room temperature (~23 °C) for 6–9 months to reach a stable crystallinity.

For preparation of pure PHB and non-PHB biomass, the microbial cells were freeze dried, dissolved in hot chloroform, and filtered to separate the polymer solution from the residual non-PHB biomass components. Pure PHB was precipitated from the chloroform solution by adding hexane, filtered and dried. The non-PHB biomass leftover from solvent extraction was oven dried at 60 °C and saved for later use.

Pure PHA samples (PHB melt, PHB film, PHB powder, and poly(3-hydroxybutyrate-*co*-3-hydroxyvalerate-*co*-4-hydroxyvalerate) (PHBVV) film) were prepared from various cell slurries (not discussed in this work), and used as generic standards of different crystallinity to calibrate ATR-FTIR spectral measurements with DSC crystallinity measurements. The PHB melt was prepared by melting pure PHB at 180 °C. The PHB film was prepared by dissolving pure PHB in hot chloroform and casting the solution on a clean glass surface as a thin film (~0.2 mm). The PHB powder and the PHBVV film were extracted and purified from different cell slurries using proprietary methods not important to the details of this work. All the pure PHA samples prepared by our research group were determined to be at least 99% pure via HPLC analysis. Biopolyesters were also purchased from Sigma-Aldrich for comparison.

2.2. Chemical analysis

The PHB content of the microbial cells was determined via acid-catalyzed methanolysis of the biopolyester in methanol (3 wt.% H_2SO_4) at 100 °C for 8–10 h (Hesselmann et al., 1999). The resulting 3-hydroxybutyric methyl ester was hydrolyzed into 3-hydroxybutyric acid at pH 11 with 10 N NaOH. The liquid samples were analyzed at 210 nm using an HPLC equipped with a UV detector (Shimazu, Japan) and an organic acid column (OA-1000, Alltech, Deerfield, IL) maintained at 65 °C and eluted with a sulfuric acid solution (pH 2) at 0.8 mL/min.

2.3. ATR-FTIR spectroscopy

The infrared absorption spectra of the pure PHA samples, PHB-containing cells, non-PHB biomass, and water were recorded with a Nicolet Avatar 370 FTIR spectrometer (Thermo Electron Co., Madison, WI). All measurements were taken in ambient conditions on a germanium crystal window of micro-horizontal attenuated total reflectance (ATR). A total of 32 scans were averaged for the measurement of a single sample over 1 min.

For measurements of the PHB film, PHB powder, and PHBVV film, the solid samples were pressed directly onto the ATR window and the absorption spectra were recorded. For measurements of the PHB melt, pure PHB was melted at 180 °C, then removed from the heat source and immediately placed on the ATR window to record its absorption spectra before significant cooling occurred. For accuracy, each of these measurements were repeated and averaged over 18 samples.

For in situ measurements of the PHB-containing cells, a small drop (~2 μL) of aqueous solution was placed directly on the ATR window and allowed to evaporate. During water evaporation, the PHB-containing cells deposited onto the ATR window via sedimentation. The total

absorption spectra, encompassing that of PHB, non-PHB biomass and water, were collected every 1–2 min for the duration (0–60 min) of the evaporation/sedimentation process.

To account for background interference caused by non-PHB biomass and water, samples of dried non-PHB biomass were wetted with varying fractions of deionized water (0–100%). The wet non-PHB biomass samples were placed directly on the ATR window and each absorption spectrum was collected immediately before significant evaporation occurred.

2.4. Differential scanning calorimetry

Thermal properties of pure PHA samples were examined via differential scanning calorimetry (DSC). A Modulated 2920 instrument (TA Instruments, New Castle, DE) equipped with a refrigerated cooling system was run in a heat–cool–heat cycle at a rate of 5 °C/min in nitrogen. The selected temperature range was 30–210 °C with sample weights of 4.5–5.5 mg.

2.5. Transmission electron microscopy

The transmission electron microscopy (TEM) images were viewed on a LEO 912 EFTEM (Zeiss, Germany) at 100 kV and photographed with a frame-transfer CCD camera (Proscan, Germany). The cells were fixed with glutaraldehyde and calcium chloride in a sodium cacodylate buffer, then post-fixated with osmium tetroxide, stained with uranyl acetate, dehydrated with ethanol and embedded in epoxy. Ultrathin (60–80 nm) sections were obtained on an Ultracut E ultramicrotome (Reichert, Austria), double stained with uranyl acetate and lead citrate.

3. Results and discussion

3.1. Monitoring the in situ crystallization of native PHB granules with ATR-FTIR

The native PHB-containing cells stored in acidic solution (pH 2) exhibited no biological activity. As seen in Fig. 1, the mild acidic conditions caused some damage to the cell walls, but did not significantly change the nature of the native PHB granules.

Fig. 2 shows a time development of the infrared absorption spectra of the native PHB granules in *R. eutropha* cells suspended in acidic solution (pH 2). In 30 min of measurement, a spectral pattern emerged due to water evaporation and cell sedimentation. Initially, the absorption spectrum of the solution was dominated by water (dotted line). As water evaporated after approximately 10 min, a secondary spectrum of the PHB granules and other cellular components emerged due to sedimentation (solid line). This spectrum may represent the instantaneous crystallinity of the native granules. After 30 min, the spectra changed due to excess dehydration, becoming fully developed, and may no longer represent the true, instantaneous crystallinity of the granules (dashed line).

According to water evaporation, the in situ measurements shown in Fig. 2 can be divided into three distinct stages. Fig. 3 contains illustrations of the three stages (initial, secondary, and final) and a plot of the infrared absorption versus measurement time at the representative wavenumbers 1184, 1226, 1278, and 1382 cm^{-1}. The wavenumbers 1184, 1226, and 1278 cm^{-1} correspond to the asymmetric stretching of the C–O–C backbone in the amorphous phase, the asymmetric stretching of the C–C–O bond in the crystalline phase due to the formation of helical chains, and the CH_2 wagging of the C–C–O backbone in the crystalline phase of PHB, respectively (Bloembergen et al., 1986; Cheng et al., 2009; Conti et al., 2006; Furukawa et al., 2005; Padermshoke et al., 2005; Sato et al., 2004; Wu et al., 2001; Xu et al., 2002; Zhang et al., 2005). The wavenumber 1382 cm^{-1} corresponds to the symmetric bending of the CH_3 group in PHB and is taken as a reference peak that is proportional to the concentration of PHB measured (Bloembergen et al., 1986). Although the reference peak 1382 cm^{-1} may experience a small change in bandwidth and a low-frequency shift during the secondary and final stages of measurement, the absorption intensity at 1382 cm^{-1} was nearly constant during these stages as seen in Figs. 2 and 3. Furthermore, the small change of absorption intensity at 1382 cm^{-1} during the secondary and final stages is negligible when compared to the intensity changes that occur at 1184, 1226, and 1278 cm^{-1}. Therefore, the absorption intensity measured at 1382 cm^{-1} can be considered insensitive to the degree of crystallinity of PHB, as previously stated by Bloembergen et al. (1986). By scaling the absorption intensities measured at 1184, 1226, and 1278 cm^{-1}

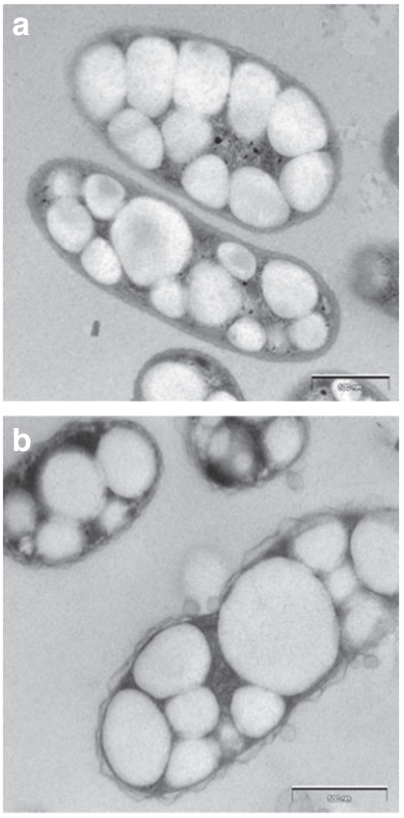

Fig. 1. Transmission electron microscopy images of *Ralstonia eutropha* cells containing PHB granules: (a) in neutral solution (pH 7) and (b) in acidic solution (pH 2). Scale bars are 500 nm.

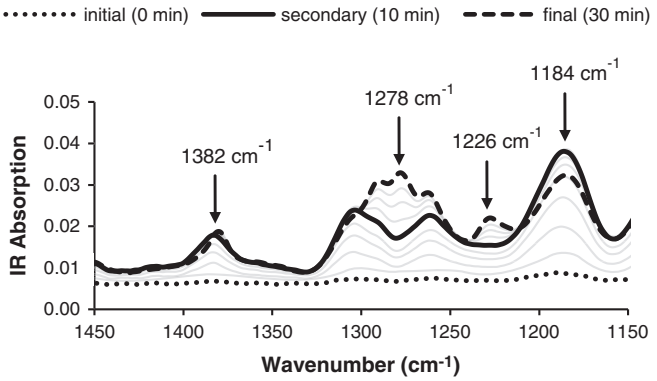

Fig. 2. Time development of the infrared absorption spectra of PHB-containing cells suspended in acidic solution (pH 2) illustrating the initial spectrum dominated by water at 0 min (dotted line), the secondary spectrum characteristic of the instantaneous crystallinity after 10 min (solid line), and the final spectrum caused by extensive dehydration after 30 min (dashed line).

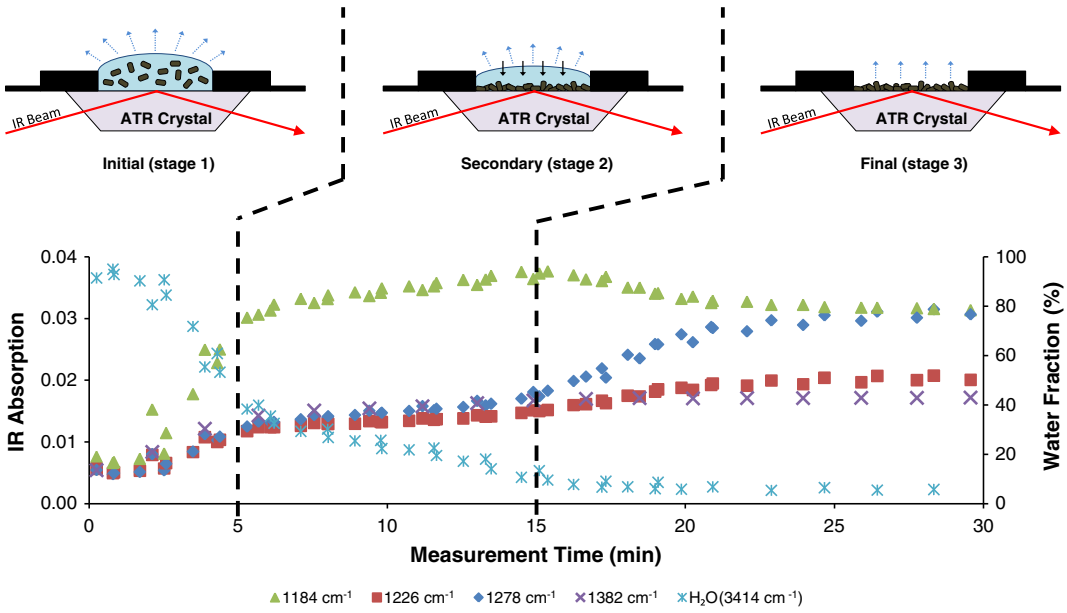

Fig. 3. Infrared absorption and water fraction of PHB-containing cells suspended in acidic solution (pH 2) versus measurement time at wavenumbers 1184, 1226, 1278, and 1382 cm^{-1}, illustrating three temporal regions: initial (stage 1), where PHB-containing cells were suspended in aqueous solution and free-water began to evaporate (0–5 min); secondary (stage 2), where free-water continued to evaporate and PHB-containing cells deposited onto the ATR window via sedimentation (5–15 min); and final (stage 3), where excess intra-granule water evaporated causing the PHB granules to crystallize (15–30 min).

with the reference peak 1382 cm^{-1}, a value known as the crystallinity index ($CI_{\tilde{\nu}}$) can be found using Eq. 1:

$$CI_{\tilde{\nu}} = \frac{A_{\tilde{\nu}}}{A_{1382}} \quad (1)$$

where $A_{\tilde{\nu}}$ is the absorption intensity measured at wavenumber $\tilde{\nu}$ and A_{1382} is the absorption intensity measured at the reference peak 1382 cm^{-1}. Also shown in Fig. 3 is data collected at the wavenumber 3414 cm^{-1}, an absorption band representative of O–H stretching present in water (Smith, 1999; Tang and Wu, 2008). The intensity at 3414 cm^{-1} can be used to estimate the relative fraction of water measured in the sample by scaling its absorbance to that of pure water.

Referring to Fig. 3, in stage 1 (0–5 min) the cells were initially suspended in water, and the infrared signal was predominated by water. As a result, very little spectral absorption by the granules was observed, which may result in unreliable, scattered measurements of the crystallinity index. In stage 2 (5–15 min) the PHB-containing cells settled down onto the ATR window and a stable region of the infrared absorbance reflecting the instantaneous crystallinity was observed. In stage 3 (15–30 min), excess dehydration of the PHB-containing cells caused the granules to further crystallize as seen by the divergence of infrared absorbance measured at the representative wavenumbers. Obviously, the absorption measurements in the final stage do not reflect the true, instantaneous crystallinity of the native granules. In other words, the increased crystallinity of the native granules in the final stage may have been artificially induced by excess dehydration.

From the illustrations and the corresponding spectral absorbance in Figs. 2 and 3, it is apparent that water played a key role in stabilizing the native PHB granules. Free-water, water surrounding the cells and possibly water in the cytosol of the cells, quickly evaporated without changing the crystallinity of the native PHB granules in stage 1 and stage 2 of Fig. 3. After some time, the PHB-bound water that resided inside the granules began to evaporate causing the granules to crystallize in stage 3 of Fig. 3. Therefore, the temporal region of interest is the secondary spectrum, as shown with the solid line in Fig. 2 and stage 2 of Fig. 3, representing the instantaneous crystallinity of the PHB granules.

The crystallinity of the native PHB granules is most conveniently monitored at the wavenumber 1184 cm^{-1}. As seen in Fig. 3, the infrared absorption at 1184 cm^{-1} is much greater than those at 1226 and 1278 cm^{-1}. Additionally, the absorption measured at 1184 cm^{-1} increases during the secondary stage (stage 2), then decreases during the final stage (stage 3). The slight increase seen in stage 2 is attributed to the evaporation of free-water, while the decreasing absorption seen in stage 3 is attributed to the artificial crystallization of PHB induced by the evaporation of intra-granule water. In contrast, the absorbance observed at 1226 and 1278 cm^{-1} is small, nearly equal to the reference peak 1382 cm^{-1}, and so, more affected by background interference. Moreover, the transition from stage 2 to stage 3 is less apparent at 1226 and 1278 cm^{-1} because the absorbance at these wavenumbers continually increases throughout the measurement process (stages 1–3). For these reasons, the wavenumber 1184 cm^{-1} is best suited to reflect the actual, in situ crystallinity of the native granules in the microbial cells.

3.2. Calculating the instantaneous crystallinity index of native PHB granules

As previously stated, the instantaneous crystallinity of native PHB granules can be measured via ATR-FTIR during the secondary stage of measurement at the wavenumber 1184 cm^{-1}. Beyond the mechanistic affect of water, vibrational energy absorbed by water generates some degree of background interference in the absorption spectra of the aqueous solution of cells. Non-PHB biomass present in the solution also causes background interference in the signal. Therefore, the total absorption spectra observed in Fig. 2 includes infrared absorptions from PHB, non-PHB biomass, and water. These components were determined to be additive as seen in Eq. 2:

$$A_{PHB\tilde{\nu}} = A_{total\tilde{\nu}} - (x \cdot A_{biomass\tilde{\nu}} + y \cdot A_{water\tilde{\nu}}) \quad (2)$$

where $A_{m\tilde{\nu}}$ is the infrared absorption of component m at wavenumber $\tilde{\nu}$, and x and y are the weight fractions of the non-PHB biomass and water, respectively.

To further investigate the background interference, the absorption spectra of dried non-PHB biomass wetted with varying fractions of water were collected. As seen in Fig. 4, the infrared absorbance of the wet non-PHB biomass was nearly constant with increasing water

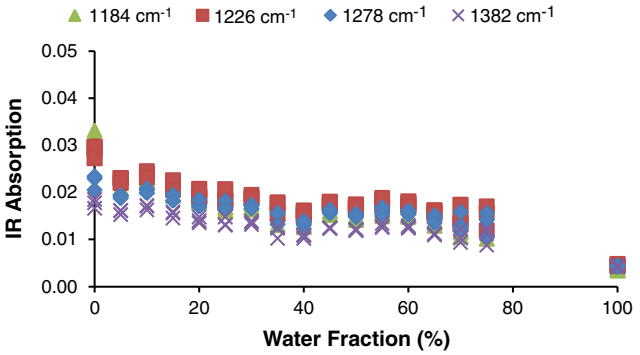

Fig. 4. Infrared absorption of non-PHB biomass wetted with varying fractions of water measured at wavenumbers 1184, 1226, 1278, and 1382 cm^{-1}.

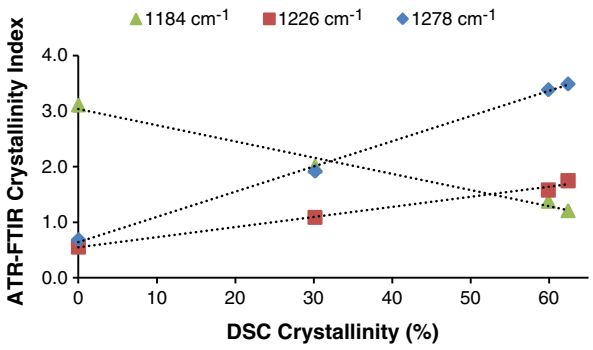

Fig. 5. ATR-FTIR crystallinity indices ($CI_{\tilde{\nu}}$) measured at the representative wavenumbers 1184, 1226, and 1278 cm^{-1} versus true crystallinity (X) measured via DSC of pure PHA samples.

fractions, particularly in the range of 30–70%, where the infrared absorption measured in this range was determined to be 0.0140 ± 5% at 1184 cm^{-1}. Thus, the background interference was assumed constant, so that Eq. 2 can be reduced to:

$$A_{PHB\,\tilde{\nu}} = A_{total\,\tilde{\nu}} - A_{background\,\tilde{\nu}} \tag{3}$$

where

$$A_{background\,\tilde{\nu}} = (x \cdot A_{biomass\,\tilde{\nu}} + y \cdot A_{water\,\tilde{\nu}}) \cong \text{constant}.$$

The background inference shown in Fig. 4, however, does not include infrared signals absorbed by PHB. Since it is impossible to know exactly what percentage of PHB, non-PHB biomass, and water was detected during measurements of the total absorption spectra, the background absorption was scaled by 50% for convenience, such that $A_{background\,1184} = 0.0070$. This estimation is valid based on the assumption that the total absorption spectra of interest (i.e., stage 2 and stage 3) contain approximately 10–30% water and 70–90% cells containing 60 wt.% PHB. Therefore, the concentration of background interference detected by the infrared signal is likely 50% (i.e., 80%×60% = 48% ≈ 50%).

Applying the same principle as in Eq. 1, the instantaneous crystallinity index at 1184 cm^{-1} can be calculated from Eq. (4):

$$CI_i = \frac{A_{PHB\ 1184}}{A_{PHB\ 1382}} = \frac{A_{total\ 1184} - A_{background\ 1184}}{A_{total\ 1382} - A_{background\ 1382}} \tag{4}$$

where CI_i is the instantaneous crystallinity index that reflects the instantaneous crystallinity of the native PHB granules measured during the secondary stage of ATR-FTIR measurement. Depending on the estimated fraction of background interference (i.e., 50%), the infrared absorbance of PHB may vary. Variations in the instantaneous crystallinity index, however, may be negligibly small due to the scaling of background interference at both 1184 and 1382 cm^{-1}, as seen in Eq. (4).

3.3. Determining the true, in situ crystallinity of native PHB granules with DSC calibration

The crystallinity indices ($CI_{\tilde{\nu}}$) of pure amorphous PHB melted at 180 °C (PHB melt) and three pure PHA samples (PHB film, PHB powder, and PHBVV film) were calculated from ATR-FTIR measurements using Eq. 1. The presumed, true crystallinity (X) of the same three PHA samples was determined via DSC using Eq. (5):

$$X = \frac{\Delta H_m}{\Delta H^0_{PHB}} \tag{5}$$

where ΔH_m is the measured enthalpy of melting of the sample and ΔH^0_{PHB} is the theoretical enthalpy of melting of pure crystal PHB (146 J/g) (Barham et al., 1984; Gunaratne et al. 2004). The true crystallinity in Eq. 5 is a theoretical prediction of its actual crystallinity as it exists in reality, which is a measure of the energy required to melt or disorder the fraction of PHB molecules vibrating in the crystalline phase.

Fig. 5 contains a plot of the true crystallinity (X) measured via DSC versus the crystallinity indices ($CI_{\tilde{\nu}}$) measured via ATR-FTIR at the representative wavenumbers 1184, 1226, and 1278 cm^{-1} of the pure PHA samples. As seen in Fig. 5, the true crystallinity is linearly correlated to the crystallinity indices following Eq. (6):

$$X = m(CI_{\tilde{\nu}}) + b \tag{6}$$

where m is the slope and b is the intercept of the calibration lines. This empirical correlation is reasonable because the crystallinity index is a measure of the number of molecules that are vibrating in the relative amorphous and crystalline phases, not a measure of molecular concentration. That is, the crystallinity index is directly proportional to the fraction of molecules vibrating in the crystalline phase. And, the true crystallinity (Eq. 5) is directly proportional to the fraction of energy required to melt the crystalline phase. Table 1 contains values of the crystallinity indices ($CI_{\tilde{\nu}}$) measured via ATR-FTIR at the representative wavenumbers 1184, 1226, and 1278 cm^{-1}, the true crystallinity measured via DSC (X), the melting temperature (T_m), and enthalpy of melting (ΔH_m) for the pure PHA samples used in this experimental method.

Eq. (6) was used to determine the true, in situ crystallinity of the native PHB granules from ATR-FTIR measurements at the wavenumber 1184 cm^{-1}, where the slope $m = -2.91$, the intercept $b = 3.04$, and the corresponding correlation coefficient squared $R^2 = 0.9842$. Rewriting Eq. 6, the instantaneous crystallinity (X_i) of the native PHB granules was calculated from the instantaneous crystallinity index (CI_i) as shown in Eq. (7):

$$X_i = -2.91(CI_i) + 3.04 \tag{7}$$

where the instantaneous crystallinity index was measured at 1184 cm^{-1} during the stable, secondary stage of the in situ ATR-FTIR measurements.

Table 1
Experimental values for the ATR-FTIR crystallinity index ($CI\tilde{\ }\nu$), true crystallinity (X), and thermal properties (T_m, ΔH_m) of pure PHA samples.

Sample	CI_{1184}	CI_{1226}	CI_{1278}	X (%)	T_m (°C)	ΔH_m (J g^{-1})
PHB film	1.21	1.75	3.49	62.4	178.1	91.1
PHB powder	1.38	1.58	3.39	59.9	173.8	87.4
PHBVV film	2.01	1.09	1.92	30.1	97.4	44.0
PHB melt	3.11	0.55	0.69	0.0	–	–

3.4. Measuring the instantaneous crystallinity of PHB granules of varying crystallinity

Fig. 6 shows the in situ crystallinity of three types of PHB-containing cells in aqueous solution of varying granule crystallinity (*native granules*, *centrifuged granules*, and *heated granules*) measured at the wavenumber 1184 cm^{-1}. As mentioned above, the instantaneous crystallinity was measured via ATR-FTIR during the secondary stage, after the initial scattering stage and before the final artificial stage. Table 2 shows average values of the total infrared absorption (A_{total}), the PHB absorption (A_{PHB}), the instantaneous crystallinity index (CI_i), and the instantaneous crystallinity (X_i) for each of the three solutions measured at 1184 cm^{-1}.

Fig. 6a shows the in situ crystallization of the native granules suspended in acidic solution (pH 2). In this figure there are three stages corresponding to the same three stages displayed in Fig. 3. In the first 5 min after the sample was placed on the ATR window, the fraction of water detected by the infrared beam was very high (60–90%). As a result, data in the initial stage (0–5 min) describing PHB crystallinity was scattered and unreliable. After 5–15 min, a significant amount of free-water evaporated and the water fraction of the signal was reduced to around 30–70%. In this secondary stage (5–15 min) the signal representative of PHB crystallinity stabilized and the instantaneous crystallinity (X_i) could be observed. Lastly, after 15–30 min the PHB crystallinity increased up to 32%, with a corresponding water content of less than 20%. When compared to the crystallization of pure PHB (Zhang et al., 2005), the final stage (15–30 min) of the native granules followed a similar trend. The instantaneous crystallinity of the native granules averaged over the secondary stage (5–15 min) was 4.89 ± 1.84% (see Table 2).

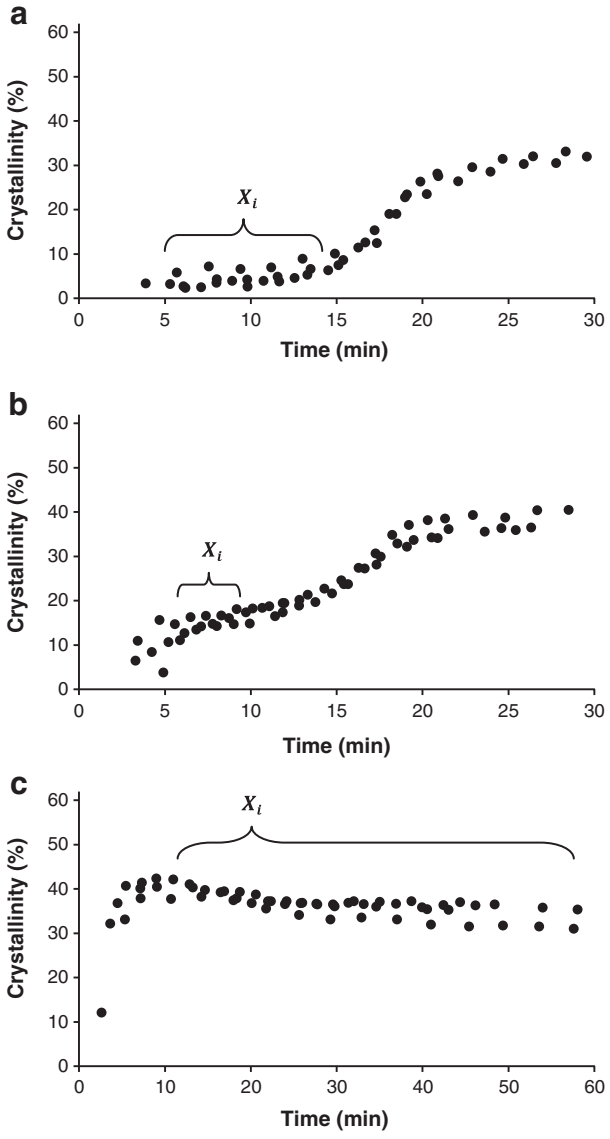

Fig. 6. In situ crystallinity versus measurement time for PHB granules: (a) native granules in acidic solution (pH 2), (b) centrifuged granules at 10,000 *g* for 1 h, and (c) heated granules at 140 °C for 2 h.

Table 2
ATR-FTIR measurements of PHB granules of varying crystallinity measured at 1184 cm^{-1} during the secondary stage of in situ measurement.

Sample	A_{total}	A_{PHB}[a]	CI_i	$X_i \pm$ STD (%)
Native granules	0.0338	0.0268	2.90	4.89 ± 1.84
Centrifuged granules	0.0292	0.0222	2.62	14.29 ± 1.78
Heated granules	0.0238	0.0168	1.98	36.33 ± 2.53

[a] Background absorption subtracted from total absorption was 0.0070.

Fig. 6b shows the in situ crystallization of the centrifuged granules spun at 10,000 *g* for 1 h. Similar to Fig. 6a, the plot of the centrifuged granules (Fig 6b) shows three temporal stages: an initial scattered stage due to high water content (0–5 min), a stable stage representing the true, instantaneous crystallinity of the granules (5–10 min), and a final stage portraying the artificial crystallization caused by excess dehydration (10–30 min). The instantaneous crystallinity of the centrifuged granules averaged over the secondary stage (5–10 min) was 14.29 ± 1.78% (see Table 2).

Fig. 6c shows the in situ crystallization of the heated granules subjected to 140 °C for 2 h. In contrast to Fig. 6a and b, the plot of the heated granules (Fig. 6c) does not contain three temporal stages. Although there was an initial scattered stage due to high water content (0–5 min), there did not seem to be separate secondary and final stages, as observed in the native and centrifuged granules. This phenomenon may be due to a change in solution density caused by heating. As a result, hydrated granules containing intra-granule water may have been trapped beneath dehydrated granules during the sedimentation process, and unable to fully dehydrate, exhibiting no final artificial crystallization stage. Regardless, the instantaneous crystallinity of the heated granules averaged over the stable region (10–60 min) was 36.33 ± 2.53% (Table 2).

Based on the observations above, the average instantaneous crystallinity of the native granules, the centrifuged granules, and the heated granules were found to be 4.89%, 14.29%, and 36.33%, respectively (see Table 2). It is widely accepted that PHB granules are fully amorphous in vivo having a crystallinity of 0% in a neutral aqueous solution (pH 7) (Barnard and Sanders, 1989; Horowitz and Sanders, 1994; Sudesh et al., 2000). When partially isolated and/or subjected to varying environmental conditions, however, the PHB granules are known to undergo varying degrees of partial crystallization (Horowitz and Sanders, 1994; Sudesh et al., 2000). As expected, the mild acidic solution (pH 2) used to store the PHB-containing cells triggered very minuscule changes in crystallinity (~5%). It seems that the intra-granule water and granule membranes remained largely intact, stabilizing the native PHB granules in a mostly amorphous state. When centrifuged (10,000 *g*, 1 h) the granules crystallized to a greater extent (~15%). This result agrees with the belief that centrifugation may induce partial crystallization due to the close packing and subsequent inactivation of PHB granules (Horowitz and Sanders, 1994; Jendrossek, 2007). In harsh conditions (140 °C, 2 h) the granules underwent a significant amount of crystallization (~35%). It seems that high temperature, not only removes some granule membranes and intra-granule water, but may also change the intra- and intermolecular arrangement of the PHB molecules within the granules. In all three aqueous solutions (native granules, centrifuged granules, and heated granules) any artificial crystallization due to

excess dehydration did not exceed 45%. The remaining granule membranes and lingering water after 30–60 min of dehydration obviously kept the PHB granules from reaching their fully crystalline state (~60%).

4. Conclusions

ATR-FTIR is a convenient method to measure the in situ crystallinity of native PHB granules accumulated within microbial cells suspended in an aqueous solution. No sample preparation, such as purification or drying, is necessary for measurement. The instantaneous crystallinity of the biopolyester granules is measured during a stable, secondary stage of infrared absorption, after an initial stage (0–5 min) where the infrared signal is dominated by water, and before a final stage (30+ min) where excess dehydration may cause the granules to artificially crystallize. Although a few representative wavenumbers may be used to monitor PHB crystallization, the wavenumber 1184 cm^{-1} is most sensitive to conformational changes present in native PHB granules. For convenience, background interference caused by water and non-PHB biomass was assumed constant regardless of the measurement time and intrinsic crystallinity. The instantaneous crystallinity (X_i) of native PHB granules was calculated by the empirical equation:

$$X_i = -2.91\, CI_i + 3.04$$

where CI_i is the instantaneous crystallinity index measured at the wavenumber 1184 cm^{-1}, during the secondary stage of ATR-FTIR measurement.

With this method it is possible to monitor the in situ crystallization behavior of native PHB granules in varying environmental conditions. Various physical and chemical treatments (i.e., changes in pH, temperature, and centrifugal force) used to extract and purify PHB may cause the native granules to undergo varying degrees of crystallization, particle aggregation, and molecule degradation. Observing the crystallization of PHB granules in different environments may help researchers understand the driving forces behind PHB crystallization and the environmental factors present that inhibit the crystallization of PHB in vivo. New recovery techniques utilizing the in situ crystallization kinetics of PHB granules may be designed to optimize particle aggregation and limit molecule degradation, while increasing PHB purity and yield — increasing efficiency and reducing the cost of PHB production.

Acknowledgments

The work is partially supported by the Consortium for Plant Biotechnology Research (CPBR) and Department of Energy. The authors appreciate the DSC analysis in Dr. Qiang Liu's laboratory, Agriculture and Agri-Food, Canada.

References

Anderson, A.J., Dawes, E.A., 1990. Occurrence, metabolism, metabolic role, and industrial uses of bacterial polyhydroxyalkanoates. Microbiol. Rev. 54, 450–472.
Barham, P.J., Keller, A., Otun, E.L., Holmes, P.A., 1984. Crystallization and morphology of a bacterial thermoplastic: poly-3-hydroxybutyrate. J. Mater. Sci. 19, 2781–2794.
Barnard, G.N., Sanders, J.K.M., 1989. The Poly-β-hydroxybutyrate granule *in vivo*: a new insight based on NMR spectroscopy of whole cells. J. Biol. Chem. 264, 3286–3291.
Bloembergen, S., Holden, D.A., Hamer, G.K., Bluhm, T.L., Marchessault, R.H., 1986. Studies of composition and crystallinity of bacterial poly(β-hydroxybutyrate-*co*-β-hydroxyvalerate). Macromolecules 19, 2865–2871.
Byrom, D., 1994. Polyhydroxyalkanoates. In: Mobley, D.P. (Ed.), Plastic from Microbes: Microbial Synthesis of Polymers and Polymer Precursors. Hanser, Munich, pp. 5–33.
Cheng, M.-L., Sun, Y.-M., Chen, H., Jean, Y.C., 2009. Change of structure and free volume properties of semi-crystalline poly(3-hydroxybutyrate-co-3-hydroxyvalerate) during thermal treatments by positron annihilation lifetime. Polymer 50, 1957–1964.
Conti, D.S., Yoshida, M.I., Pezzin, S.H., Coelho, L.A.F., 2006. Miscibility and crystallinity of poly(3-hydroxybutyrate)/poly(3-hydroxybutyrate-*co*-3-hydroxyvalerate) blends. Thermochim. Acta 450, 61–66.
Cornibert, J., Marchessault, R.H., 1975. Conformational isomorphism. A general 2_1 helical conformation for poly(β-alkanoates). Macromolecules 8, 296–305.
Furukawa, T., Sato, H., Murakami, R., Zhang, J., Duan, Y.-X., Noda, I., Ochiai, S., Ozaki, Y., 2005. Structure, dispersibility, and crystallinity of poly(hydroxybutyrate)/poly(L-lactic acid) blends studied by FT-IR microspectroscopy and differential scanning calorimetry. Macromolecules 38, 6445–6454.
Grage, K., Jahns, A.C., Parlane, N., Palanisamy, R., Rasiah, I.A., Atwood, J.A., Rehm, B.H.A., 2009. Bacterial polyhydroxyalkanoate granules: biogenesis, structure, and potential use as nano-/micro-beads in biotechnology and biomedical applications. Biomacromolecules 10, 660–669.
Gunaratne, L.M.W.K., Shanks, R.A., Amarasinghe, G., 2004. Thermal history effects on crystallisation and melting of poly(3-hydroxybutyrate). Thermochim. Acta 423, 127–135.
Hesselmann, R.P.X., Fleischmann, T., Hany, R., Zehnder, A.J.B., 1999. Determination of polyhydroxyalkanoates in activated sludge by ion chromatographic and enzymatic methods. J. Microbiol. Methods 35, 111–119.
Horowitz, D.M., Sanders, J.K.M., 1994. Amorphous, biomimetic granules of polyhydroxybutyrate: preparation, characterization, and biological implications. J. Am. Chem. Soc. 116, 2695–2702.
Jendrossek, D., 2007. Peculiarities of PHA granule preparation and PHA depolymerase activity determination. Appl. Microbiol. Biotechnol. 74, 1186–1196.
Padermshoke, A., Katsumoto, Y., Sato, H., Ekgasit, S., Noda, I., Ozaki, Y., 2005. Melting behavior of poly(3-hydroxybutyrate) investigated by two-dimensional infrared correlation spectroscopy. Spectrochim. Acta, Part A 61, 541–550.
Sato, H., Murakami, R., Padermshoke, A., Hirose, F., Senda, K., Noda, I., Ozaki, Y., 2004. Infrared spectroscopy studies of CH···O hydrogen bondings and thermal behavior of biodegradable poly(hydroxyalkanoate). Macromolecules 37, 7203–7213.
Smith, B., 1999. Infrared Spectral Interpretation: A Systematic Approach. CRC Press, Boca Raton.
Stuart, E. S., Tehrani A., Valentin H. E., Dennis D., Lenz R. W., Fuller R. C., 1998. Protein organization on the PHA inclusion cytoplasmic boundary. J. Biotechnol. 64, 137-144.
Sudesh, K., Abe, H., Doi, Y., 2000. Synthesis, structure and properties of polyhydroxyalkanoates: biological polyesters. Prog. Polym. Sci. 25, 1503–1555.
Tang, B., Wu, P., 2008. In situ study of diffusion and interaction of water and electrolyte solution in polyacrylonitrile (PAN) membrane using FTIR and two-dimensional correlation analysis. Vib. Spectrosc. 1665, 1–7.
Wu, Q., Tian, G., Sun, S., Noda, I., Chen, G.-Q., 2001. Study of microbial polyhydroxyalkanoates using two-dimensional Fourier-transform infrared correlation spectroscopy. J. Appl. Polym. Sci. 82, 934–940.
Xu, J., Guo, B.-H., Yang, R., Wu, Q., Chen, G.-Q., Zhang, Z.-M., 2002. In situ FTIR study on melting and crystallization of polyhydroxyalkanoates. Polymer. 43, 6893–6899.
Zhang, J., Sato, H., Noda, I., Ozaki, Y., 2005. Conformation rearrangement and molecular dynamics of poly(3-hydroxybutyrate) during the melt-crystallization process investigated by infrared and two-dimensional infrared correlation spectroscopy. Macromolecules. 38, 4274–4281.